

Materially & Geometrically Nonlinear Woven Composite Micro-mechanical Model with Failure for Finite Element Simulations

Ala Tabiei* and Ivelin Ivanov†

Department of Aerospace Engineering and Engineering Mechanics
University of Cincinnati, OH 45221-0070, USA

ABSTRACT

A computational micro-mechanical material model of woven fabric composite material is developed to simulate failure. The material model is based on repeated unit cell approach. The fiber reorientation is accounted for in the effective stiffness calculation. Material non-linearity due to the shear stresses in the impregnated yarns and the matrix material is included in the model. Micro-mechanical failure criteria determine the stiffness degradation for the constituent materials. The developed material model with failure is programmed as user defined subroutine in the LS-DYNA finite element code with explicit time integration. The code is used to simulate the failure behavior of woven composite structures. The results of finite element simulations are compared with available test results. The model shows good agreement with the experimental results and good computational efficiency required for finite element simulations of woven composite structures.

Keywords: composite material failure, computational composite material model, woven fabric composites, textile composites, fiber reorientation, and nonlinear finite element simulations.

* Associate Professor, author to whom correspondence should be addressed

† Graduate Research Assistant

Introduction

Woven composite materials are being used as primary structural components in many applications. Failure analysis of such structures is an essential part of the structure design. Along with their advantages however, the complex architecture of the woven fabric composites makes the analysis and the simulation of their failure behavior very difficult. Tremendous amount of works dedicated to the modeling of woven composites intends to predict the elastic properties of the materials and only few of them consider the failure behavior. The reason for this is the complex phenomena affecting the progressive failure behavior of woven fabric composites. These phenomena are the material nonlinearity of the matrix material combined with the geometrical nonlinearity of the fiber reorientation and the damage accumulation with stress concentration in the interacting constituents.

The unit cell approach is employed in the analysis of the most material models of woven composite structures. The composite structure is divided into repeated cells, representing the properties and the behavior of the whole lamina. The classical 1-D models of Ishikawa and Chou [1-4] were extended to 2-D elastic models by N.K. Naik et al. [5-6]. Naik and Ganesh [6] considered the failure in the fill yarn direction of loading only. Naik and Ganesh [6] divided the sub-cells of their Representative Volume Cell (RVC) into many slices. They used different failure criteria for the different constituents: Tsai-Wu failure criterion for the fill strand, maximum strain criterion for the warp strand and maximum stress criterion for the pure matrix material. After the matrix material failure in the “gap” region, the fill strand is modeled as a curved cantilever slender beam.

R.A. Naik [8] developed 3-D micro-mechanical material models of woven and braided fabric composite materials with failure. The undulated part of the yarn is discretized in many slices and a volume averaging technique based on iso-strain assumption is used to obtain the elastic properties of the RVC. Material shear nonlinearity for yarn and matrix materials is included and described by the three parametric equation of Ramberg-Osgood. The calculation of stress and strain in some directions is based on the curved beam on elastic foundation model for the undulated part of the yarns, and the straightening of the yarns is accounted for as geometrical nonlinearity in the nonlinear incremental solution. The failure criteria and the stiffness degradation scheme are presented by Blackketter et. al. [9]. Blackketter et. al. applied shear material nonlinearity and stiffness degradation to a finite element model of the woven fabric composite RVC and successfully simulated the damage propagation in tension and pure shear loadings in yarn direction. The micro-mechanical material model of R.A. Naik is incorporated in a computer code called TEXCAD, which is used for failure analysis of fabric composite materials.

Tabiei et. al. [10] suggested a micro-mechanical material model of woven fabric composite materials to simulate the progressive failure. The quarter sub-cell of the RVC is divided in many blocks. Micro-mechanical failure criteria for each constituent material in the block and corresponding stiffness degradation are adopted there. The material shear nonlinearity described by Hahn and Tsai is included in the model.

The material models of woven fabric composites described above are suitable for nonlinear finite element failure analysis of composite structures, but because of the high degree

of RVC discretization, they are computationally inefficient to be applied in explicit finite element codes. The nonlinear finite element codes with explicit time integration are very powerful for large-scale simulations but because of the inherent small time step for stable solution they require high computational efficiency of the material models. This characteristic is an obstacle for complicated micro-mechanical models to be implemented in the explicit codes. The authors developed a computationally efficient and simplified micro-mechanical model of woven fabric composite materials [11] to predict their elastic properties. The advantage of the model is the lack of RVC discretization and good elastic property prediction. The choice of the RVC is intended to account for geometrical nonlinearity and simple and efficient technique for fiber reorientation was incorporated in the model [12]. The aim of this work is to develop the already formulated micro-mechanical material model of woven fabric composites with material nonlinearity and micro-mechanical failure in order to simulate the progressive failure of woven composites in finite element simulations using the explicit time integration.

Micro-mechanical model

The micro-mechanical material model and the homogenization procedure determining the elastic properties of woven fabric composite material employed in this work are described in [11]. For the sake of completeness the model will be shortly summarized here. The RVC of the woven fabric composite material is extracted from the deformed material pattern as it is shown in Fig. 1. The architecture of the woven fabric material is modeled by two over-crossed straight broken strands in elastic media (Fig. 2). The strands represent the fill and the warp yarns, respectively and the elastic media represents the matrix material. The orientation of the yarns is described by two angles: the braid angle θ and the undulation angle β (Fig. 3). The RVC is divided in four sub-cells: two anti-symmetric sub-cells consisting the fill yarn and two anti-symmetric sub-cells consisting the warp yarn.

The homogenization procedure for elastic properties begins with the stiffness matrix of each constituent material in each sub-cell. A degradation of the elastic moduli is applied for each constituent in the different sub-cells depending on the attained stress of the constituent. When failure is detected the degradation is applied only on the elastic moduli by multiplying them with a discount factor $d_i \in (0, 1]$ (i designates the elastic modulus to which it is applied). Degradation is not applied on the Poisson's ratios. In order to obey the following relation:

$$\frac{\nu_{ij}}{E_i} = \frac{\nu_{ji}}{E_j} \quad , \quad i, j = 1, 2, 3 \quad , \quad (1)$$

the yarn material is considered as orthotropic with the following stiffness matrix [13]:

$$[C]_y = [S]_y^{-1} = \begin{bmatrix} \frac{1}{E_1} & -\sqrt{\frac{\nu_{12}}{E_1} \frac{\nu_{21}}{d_2 E_2}} & -\sqrt{\frac{\nu_{12}}{E_1} \frac{\nu_{21}}{d_3 E_2}} & 0 & 0 & 0 \\ -\sqrt{\frac{\nu_{12}}{E_1} \frac{\nu_{21}}{d_2 E_2}} & \frac{1}{d_2 E_2} & -\frac{\nu_{23}}{\sqrt{d_2 E_2 d_3 E_2}} & 0 & 0 & 0 \\ -\sqrt{\frac{\nu_{12}}{E_1} \frac{\nu_{21}}{d_3 E_2}} & -\frac{\nu_{23}}{\sqrt{d_2 E_2 d_3 E_2}} & \frac{1}{d_3 E_2} & 0 & 0 & 0 \\ 0 & 0 & 0 & \frac{1}{d_4 G_{12}} & 0 & 0 \\ 0 & 0 & 0 & 0 & \frac{1}{d_5 G_{23}} & 0 \\ 0 & 0 & 0 & 0 & 0 & \frac{1}{d_6 G_{12}} \end{bmatrix}^{-1}, \quad (2)$$

where d_i , $i = 2, 3, \dots, 6$, are the discount factors for yarn material, initially all of them equal unity, E_1, E_2, G_{12}, G_{23} and $\nu_{12}, \nu_{21}, \nu_{23}$, are the elastic moduli and Poisson's ratios of the yarn material respectively. The resin material has a simpler stiffness matrix as follows:

$$[C]_m = [S]_m^{-1} = \begin{bmatrix} \frac{1}{d_E E} & -\frac{\nu}{d_E E} & -\frac{\nu}{d_E E} & 0 & 0 & 0 \\ -\frac{\nu}{d_E E} & \frac{1}{d_E E} & -\frac{\nu}{d_E E} & 0 & 0 & 0 \\ -\frac{\nu}{d_E E} & -\frac{\nu}{d_E E} & \frac{1}{d_E E} & 0 & 0 & 0 \\ 0 & 0 & 0 & \frac{1}{d_G G} & 0 & 0 \\ 0 & 0 & 0 & 0 & \frac{1}{d_G G} & 0 \\ 0 & 0 & 0 & 0 & 0 & \frac{1}{d_G G} \end{bmatrix}^{-1}, \quad (3)$$

The Young's modulus, E , and shear modulus, G , are degraded independently by different discount factors d_E and d_G , both initially equal unity.

The elastic material properties of yarn and matrix materials are homogenized for each sub-cell and the stiffness matrix in direction of the material axes (Fig. 3) is obtained for each sub-cell at the first level of the homogenization procedure. The homogenization procedure is based on mixed, iso-strain and iso-stress, boundary conditions. The stiffness matrix of each sub-cell is transformed to the RVC coordinate system (x, y, z in Fig. 2), using the current directional braid and undulation angles of the yarns. The effective stiffness matrix of the RVC is obtained after applying the second level of the homogenization procedure. Note that because of the

different stresses in the constituents of the different sub-cells, the degradation is different and the anti-symmetry of the sub-cells cannot be exploited.

Having the effective stiffness matrix of the RVC, $[\bar{C}]_{RVC}$, we can calculate the stress response of the material model at each time step n for nonlinear explicit finite element code:

$$\{d\bar{\sigma}\} = [\bar{C}]_{RVC} \{d\bar{\varepsilon}\}, \quad (4)$$

$$\{\bar{\sigma}\}_n = \{\bar{\sigma}\}_{n-1} + \{d\bar{\sigma}\}, \quad (5)$$

where $\{d\bar{\sigma}\}$ and $\{d\bar{\varepsilon}\}$ are the stress and strain increments in the composite material respectively. In order to obtain the stress and strain in constituents one can use formulae (16) and (4) as described in [11]:

$$\{\varepsilon_s\}_k = [C_{ss}]_k^{-1} \{\bar{\sigma}_s\} - [C_{ss}]_k^{-1} [C_{sn}]_k \{\bar{\varepsilon}_n\}. \quad (6)$$

$$\{\sigma_n\}_k = [C_{nn}]_k \{\varepsilon_n\}_k + [C_{ns}]_k \{\varepsilon_s\}_k, \quad (7)$$

Then applying (6) and (7) twice, once to obtain the stress and strain increments in the four sub-cells from the stress and strain increments of RVC and then again for each sub-cell to determine the stress and strain increments in the yarn and in the matrix material from the stress and strain increments of the sub-cell. For the first calculation the following equations are applied:

$$\{\bar{\sigma}_s\} = \{\sigma_s\}_k = \{d\bar{\sigma}_3 \quad d\bar{\sigma}_5 \quad d\bar{\sigma}_6\}^T, \quad (8)$$

$$\{\bar{\varepsilon}_n\} = \{\varepsilon_n\}_k = \{d\bar{\varepsilon}_1 \quad d\bar{\varepsilon}_2 \quad d\bar{\varepsilon}_4\}^T, \quad (9)$$

where k denotes the sub-cell ($k = f, w, F, W$) and the adopted contracted notation for stress and strain components is $1 \cong 11, 2 \cong 22, 3 \cong 33, 4 \cong 12, 5 \cong 23, 6 \cong 31$. After applying (6) and (7) on (8) and (9) the iso-strain components (denoted by n) and the iso-stress components (denoted by s) of the strain and stress increment in each sub-cell, k , in the coordinate system of the RVC are obtained. Therefore, the full strain increment vector, $\{d\varepsilon'\}$, and the full stress increment vector, $\{d\sigma'\}$, are constructed for each sub-cell. These increment vectors are in the RVC coordinate system and they are transformed to the material coordinate system by means of the transformation matrix $[T]$ as reported in [11],

$$\{d\varepsilon\} = [T] \cdot \{d\varepsilon'\} = \begin{bmatrix} [T_1] & [T_2] \\ [T_3] & [T_4] \end{bmatrix} \cdot \{d\varepsilon'\}, \quad (10)$$

$$\{d\sigma\} = [T_\sigma] \cdot \{d\sigma'\} = \begin{bmatrix} [T_1] & 2[T_2] \\ \frac{1}{2}[T_3] & [T_4] \end{bmatrix} \cdot \{d\sigma'\}. \quad (11)$$

The full strain and the full stress increment vectors of each sub-cell are divided into iso-strain and iso-stress parts in order to obtain the stress and strain increments in constituent materials. The assumed iso-strain and iso-stress boundary conditions for the homogenization of the yarn and the matrix materials are as follows:

$$\{\bar{\sigma}_s\} = \{\sigma_s\}_k = \{d\sigma_2 \ d\sigma_3 \ d\sigma_5\}^T, \quad (12)$$

$$\{\bar{\epsilon}_n\} = \{\epsilon_n\}_k = \{d\epsilon_1 \ d\epsilon_4 \ d\epsilon_6\}^T, \quad (13)$$

where k now denotes the constituent materials of the sub-cell ($k = y, m$). Applying (6) and (7) but now on (12) and (13) again, all components of the strain and stress increments in the constituent materials are obtained and the full stress increment vectors in the yarn and the matrix materials can be constructed as follows:

$$\{d\sigma^y\} = \{d\sigma_1^y \ d\sigma_2^y \ d\sigma_3^y \ d\sigma_4^y \ d\sigma_5^y \ d\sigma_6^y\}^T, \quad (14)$$

$$\{d\sigma^m\} = \{d\sigma_1^m \ d\sigma_2^m \ d\sigma_3^m \ d\sigma_4^m \ d\sigma_5^m \ d\sigma_6^m\}^T. \quad (15)$$

The total stress in the constituent materials is accumulated at each time step, n , for each sub-cell and it is kept as historical variable:

$$\{\sigma^y\}_n = \{\sigma^y\}_{n-1} + \{d\sigma^y\}, \quad \{\sigma^m\}_n = \{\sigma^m\}_{n-1} + \{d\sigma^m\}. \quad (16)$$

The orientation of the fill and the warp yarns is determined in the coordinate system of RVC by the braid and the undulation angles. They are denoted by subscript f or w for the fill and the warp yarn, respectively. We can construct directional vectors for each of the yarns in order to rotate them to the new position at each time step, n , to obtain the updated braid and undulation angles [12]:

$$\{q_f\} = \{\cos\beta_f \cos\theta_f \quad \cos\beta_f \sin\theta_f \quad \sin\beta_f\}^T, \quad (17)$$

$$\{q_w\} = \{\cos\beta_w \cos\theta_w \quad \cos\beta_w \sin\theta_w \quad \sin\beta_w\}^T. \quad (18)$$

The directional vectors are rotated and then normalized by means of the approximate deformation gradient tensor, $[F]$:

$$\{q'_f\} = [F]\{q_f\}, \quad \{q'_w\} = [F]\{q_w\}, \quad (19)$$

$$\{q_f\} = \{q'_f\} / \|\{q'_f\}\|, \quad \{q_w\} = \{q'_w\} / \|\{q'_w\}\|, \quad (20)$$

where

$$[F] = \begin{bmatrix} 1 + d\bar{\epsilon}_1 & \frac{d\bar{\epsilon}_4}{2} & \frac{d\bar{\epsilon}_6}{2} \\ \frac{d\bar{\epsilon}_4}{2} & 1 + d\bar{\epsilon}_2 & \frac{d\bar{\epsilon}_5}{2} \\ \frac{d\bar{\epsilon}_6}{2} & \frac{d\bar{\epsilon}_5}{2} & 1 + d\bar{\epsilon}_3 \end{bmatrix}. \quad (21)$$

The new orientation angles of the yarns are determined from the updated directional vectors:

$$\beta_f = \sin^{-1} q_{f3}, \quad \beta_w = \sin^{-1} q_{w3}, \quad (22)$$

$$\theta_f = \tan^{-1}(q_{f2}/q_{f1}), \quad \theta_w = \tan^{-1}(q_{w2}/q_{w1}). \quad (23)$$

Initially, $\beta_f = \beta_w = \beta_0$, $\theta_f = 45^\circ$, $\theta_w = -45^\circ$. Note that in this technique the orientation of the yarns depends on the global strain increment of the RVC, not on the strain increment of the sub-cells.

Material Nonlinearity

The shear material nonlinearity of composite materials is recognized by many authors [6-10] to be important for failure analysis. Material nonlinearity could govern the behavior of woven composite material in some certain loadings. The three parameters equation of Ramberg-Osgood is adopted here to describe the shear nonlinear behavior of the constituent materials in the sub-cells:

$$\tau(\gamma) = \frac{G_0 \gamma}{\left[1 + \left(\frac{G_0 \gamma}{S} \right)^p \right]^{\frac{1}{p}}}, \quad (24)$$

where G_0 is the initial shear modulus, S is the ultimate shear strength, and p is a shape parameter which can be determined by a curve-fit to experimental shear stress-strain data.

In the incremental solution of the nonlinear finite element method, the tangential shear modulus is used in the constitutive equations relating the stress and strain increments as follows:

$$d\tau = G_t d\gamma, \quad (25)$$

where $G_t = \frac{d\tau}{d\gamma}$ is the tangential shear modulus. The tangential shear modulus can be obtained as a function of the shear strain, $G_t \equiv G_t(\gamma)$, by differentiating equation (24). In the presented material model of woven fabric composite materials, the total stress components of the constituent materials are calculated only for failure analysis and they are kept as history variables for further accumulation and analysis. The total shear strain components are missing, so that the

tangential shear modulus as a function of the shear stress, $G_t \equiv G_t(\tau)$, has to be derived. The inverse function, $\gamma \equiv \gamma(\tau)$, can be easily found from (24) as follows:

$$\gamma(\tau) = \frac{\tau}{G_0 \left[1 - \left(\frac{\tau}{S} \right)^p \right]^{\frac{1}{p}}} \quad (26)$$

and then the tangential shear modulus can be obtained:

$$G_t = \frac{1}{\frac{d\gamma}{d\tau}} = G_0 \left[1 - \left(\frac{\tau}{S} \right)^p \right]^{1 + \frac{1}{p}}. \quad (27)$$

The shear material nonlinearity can be introduced in the material model as discount factors for the shear moduli from equation (27):

$$d_s = \frac{G_t}{G_0}. \quad (28)$$

The instantaneous discount factors for the shear material nonlinearity of the yarn material, d_{s4} , d_{s5} and d_{s6} , are calculated from the stress components σ_4^y , σ_5^y and σ_6^y , respectively by the following formulae:

$$d_{s4} = \left[1 - \left(\frac{\sigma_4^y}{S_l} \right)^{p_y} \right]^{1 + \frac{1}{p_y}}, \quad d_{s5} = \left[1 - \left(\frac{\sigma_5^y}{S_t} \right)^{p_y} \right]^{1 + \frac{1}{p_y}}, \quad d_{s6} = \left[1 - \left(\frac{\sigma_6^y}{S_l} \right)^{p_y} \right]^{1 + \frac{1}{p_y}}, \quad (29)$$

where p_y is the shape parameter of Romberg-Osgood equation and S_l and S_t are the longitudinal and transverse shear strength of the yarn material, respectively. Similarly, the instantaneous shear discount factor for the matrix material, d_{sG} , is calculated from the octahedral shear stress, τ_o :

$$d_{sG} = \left[1 - \left(\frac{\sqrt{\frac{3}{2}} \tau_o}{S} \right)^{p_m} \right]^{1 + \frac{1}{p_m}}, \quad (30)$$

where p_m is the shape parameter for the matrix material, S is the shear strength and the octahedral shear stress is calculated from the stress components of the matrix material by using the following formula:

$$\tau_o = \frac{1}{3} \sqrt{(\sigma_1^m - \sigma_2^m)^2 + (\sigma_2^m - \sigma_3^m)^2 + (\sigma_3^m - \sigma_1^m)^2 + 6(\sigma_4^m + \sigma_5^m + \sigma_6^m)}. \quad (31)$$

Note that when explicit time integration is utilized the material stiffness matrix is updated with relatively high frequency and consequently the material nonlinearity is properly captured.

Failure criteria and stiffness degradation

The failure criteria and stiffness degradation scheme is adopted almost entirely from Blacketter et. al. [9]. The isotropic matrix material in each sub-cell is checked for failure by testing the maximum of the principle stresses, $\sigma_I^m, \sigma_{II}^m, \sigma_{III}^m$:

$$\text{if } \max\{\sigma_I^m, \sigma_{II}^m, \sigma_{III}^m\} > X_m \text{ then } d_E = 0.01, \quad d_{fG} = 0.20, \quad (32)$$

where X_m is the tensile strength of the matrix material and d_E, d_{fG} are the discount factors. The failure criteria and the degradation scheme for the yarn material are given in Table 1. The failure in the axial direction of the yarn leads to fiber breakage. This kind of failure is considered as an ultimate failure of the composite material.

Note that the stress component in the longitudinal direction of the yarn is multiplied by stress concentration factors, c_t and c_c for tension and compression respectively (see Table 1). The stress distribution in the yarn constituent is investigated in [15] and [16]. It is obvious that the adopted simplified architecture of woven fabric composites is not able to predict the stress concentration, which is important in tension and compression in the direction of yarns. It is difficult to justify the value of concentration factors with respect to the adopted material model architecture from some geometrical considerations. However, it is possible to vary the stress concentration factors in order to fit the ultimate material model failure to the experimental failure of the woven fabric composite. This should be done in tension and compression in the 0/90 degree loading.

The stress concentration factor affects the ultimate failure point in the stress-strain diagram for tension or compression in 0/90 degree loading. If there is no failure of transverse yarns in 0/90 degree loading the ultimate failure point is at about the ultimate longitudinal strain of the yarn material for stress concentration factor equals unity. Test results of woven fabric composite materials in the mentioned loading condition show that the ultimate strain in the direction of loading is quite lower than the ultimate longitudinal strain of the yarn material. This is because the failure of the undulated yarns happens earlier than that of the straight yarns in longitudinal tension. The stress concentration in the undulated yarns and the combination of tension with bending of the undulated yarns, which are like a curve beam in an elastic foundation (the matrix material), lead to the lower ultimate strain.

The behavior of woven fabric composite materials under shear for 0/90 degree loading (or +45/-45 degree tension/compression) is governed by the matrix material nonlinearity. The ultimate failure occurs as a result of high strain and the lost of integrity of the composite material. In order to predict that failure mode, an integrity failure criterion is introduced in the failure model. The total strain of the RVC is accumulated at each time step and it is kept as a history variable. The maximum principle strain and the maximum shear strain of the RVC are calculated and examined at each time step. If one of them exceeds the ultimate strain for the

integrity, E_u , an ultimate failure is assumed in the material model and the material is considered totally failed.

Numerical examples

The described micro-mechanical material model of woven fabric composite materials is programmed first in the MATLAB software. The Adopted incremental approach for nonlinear solution was similar to the one described in [12]. The Graphite/Epoxy plain-woven fabric composite material (AS4/3501-6) under tension and pure shear loadings, as it is described in [8] and [9], is considered as validation example for the developed material model with failure. The elastic and strength properties of the impregnated yarn ($V_f = 0.7$) are as follows:

$$\begin{aligned} E_1 &= 151 \text{ GPa} , E_2 = 10.1 \text{ GPa} , G_{12} = 5.7 \text{ GPa} , G_{23} = 3.4 \text{ GPa} , \\ \nu_{12} &= 0.24 , \nu_{23} = 0.5 , p = 2.78 , X_t = 2550 \text{ MPa} , X_c = 2000 \text{ MPa} , \\ Y_t &= 152 \text{ MPa} , Y_c = 206 \text{ MPa} , S_l = 97 \text{ MPa} , S_t = 55 \text{ MPa} . \end{aligned}$$

The elastic properties and the strength of the matrix material are:

$$E = 4.4 \text{ GPa} , G = 1.7 \text{ GPa} , \nu = 0.34 , p = 2.34 , X_m = 159 \text{ MPa} , S_m = 110 \text{ MPa} .$$

The total volume fraction of the fibers in the composite material is 60% and since the yarns fiber volume fraction is 70%, the volume fraction of the impregnated yarn material in the material model is considered 85.7%. The initial undulation angle of the yarns is 1 degree and the initial braid angle is 45 degree. The stress concentration factor is taken to be 1.6 for the yarns. The ultimate strain for the integrity failure is assumed to be 6%.

The material model programmed in MATLAB calculates the stress response of the woven fabric composite due to steady strain loading with a constant strain increment in tension and in pure shear. The result is compared to the experimental data from [8,9] and to the predictions from Blacketter et. al. [9] and R.Naik (TEXCAD) [8]. The result of tension loading is given in Fig. 5. The stress response to the pure shear loading is shown in Fig. 6. The material model has slightly softer behavior in shear than the experimental result similar to all other material models presented. The stress response of the material model in tension almost coincides with the experimental result.

The developed micro-mechanical material model of woven fabric composite materials is also programmed as a user defined subroutine in the LS-DYNA commercial finite element code with explicit time integration. The material model can be used for shell as well as for solid elements. Trying to justify the model in various and more complicated loadings, we found experimental data for 5-harness satin IM7/8551 7A Graphite/Epoxy in tension, compression and bending [17]. Although, the present micro-mechanical model represents the plain-woven fabric composite architecture, it is applicable for some other fabric architectures also. The undulated portion of the yarns is not discretized in details in the model and the yarns are not necessarily orthogonal. In this way, the homogenization technique applied is suitable for fabric architectures like satin woven fabrics and some of the braided fabrics.

The test specimen of the composite material is modeled by means of shell elements. The elastic properties of the yarns and their strength are as follows:

$$\begin{aligned} E_1 &= 203 \text{ GPa} , E_2 = 11.2 \text{ GPa} , G_{12} = 8.4 \text{ GPa} , G_{23} = 8.4 \text{ GPa} , \\ \nu_{12} &= 0.32 , \nu_{23} = 0.30 , X_t = 3500 \text{ MPa} , X_c = 2700 \text{ MPa} , \\ Y_t &= 56 \text{ MPa} , Y_c = 200 \text{ MPa} , S_l = 98 \text{ MPa} , S_t = 98 \text{ MPa} . \end{aligned}$$

The elastic properties and the strength of the resin epoxy are:

$$E = 3.45 \text{ GPa} , G = 1.28 \text{ GPa} , \nu = 0.35 , X_m = 84.9 \text{ MPa} , S_m = 98.3 \text{ MPa} .$$

The stress-strain curve obtained in the finite element simulation for 0/90 degree tension is compared to the experimental curve and they are shown in Fig. 7. The tensile stress versus transverse strain is given on the left side of the figure and the tensile stress versus longitudinal strain is on the right side. The stress-strain curve of the simulation in +45/-45 degree tension is very close to the experimental curve as depicted in (Fig. 8). The stress concentration factor for compression is considered to be 2.98. The stress-strain curves for 0/90 degree compression loading are given in Fig. 9. The results for +45/-45 degree compression are shown in Fig. 10. Using the adjusted in tension and compression parameters for the material model, four point bending of a specimen in 0/90 and in +45/-45 degree orientations are simulated and compared to the experimental data. The results are given in Fig. 11 and Fig. 12, respectively. The results of the simulations are in very good agreement with the experimental results.

Conclusions

A micro-mechanical material model of woven fabric composite materials with failure is developed. The model is computationally efficient and its implementation in the LS-DYNA nonlinear finite element code shows the potential of the model to be used in large-scale simulations of composite structures. The material model is augmented by geometrical nonlinearity of fiber reorientation and by shear material nonlinearity. These nonlinearities with the adopted failure criteria and stiffness degradation scheme make the model suitable for finite element simulations of composites in various and complex loadings. The material model stress prediction and failure are in very good agreement with the experimental data of woven fabric composite materials under different loadings.

Acknowledgment

Support was provided by the ACC. Computing support was provided by the Ohio Supercomputer Center. Their support is gratefully acknowledged.

References

1. T. Ishikawa, "Antisymmetric elastic properties of composite plates of satin weave cloth", *Fiber Science and Technology*, **15**, 127-145, (1981).
2. T. Ishikawa and T.W. Chou, "Elastic behavior of woven hybrid composites", *Journal of Composite Materials*, **16**, 2-19 (1982).
3. T. Ishikawa and T.W. Chou, "Stiffness and strength behavior of fabric composites", *Journal of Material Science*, **17**, 3211-3220, (1982).
4. T. Ishikawa and T.W. Chou, "One-dimensional micromechanical analysis of woven fabric composites", *AIAA Journal*, **21** (12), 1714-1721, (1983).
5. N.K. Naik and P.S. Shembekar, "Elastic behavior of woven fabric composites: I- lamina analysis", *Journal of Composite Materials*, **26** (15), 2196-2225, (1992).
6. N.K. Naik and V.K. Ganesh, "Failure behavior of plain weave fabric laminates under on-axis uniaxial tensile loading: II analytical predictions", *Journal of Composite Materials*, **30** (16), 1779-1822, (1996).
7. H.T. Hahn and S.W. Tsai, "Nonlinear elastic behavior of unidirectional composite laminae", *Journal of Composite Materials*, **7**, 102-118, (1973).
8. R.A. Naik, "Failure analysis of woven and braided fabric reinforced composites", *Journal of Composite Materials*, **29**, 2334-2363, (1995).
9. D.M. Blacketter, D.E. Walrath and A.C. Hansen, "Modeling damage in a plain weave fabric-reinforced composite material", *Journal of Composites Technology and Research*, **15** (2), 136-142, (1993).
10. A. Tabiei, G. Song, and Y. Jiang, "Strength simulation of woven fabric composite materials with material nonlinearity using micromechanics based model", submitted to *Journal of Thermoplastic Composite Materials*, (2000).
11. I. Ivanov and A. Tabiei, "Three-dimensional computational micro-mechanical model for woven fabric composites", *Composite Structures*, **54**, 4, 489-496, (2001).
12. A. Tabiei and I. Ivanov, "Fiber reorientation in unidirectional and woven composites for finite element simulation", submitted to *Composite Science and Technology*, (2001).
13. A. Tabiei and J. Wu, "Three-dimensional nonlinear orthotropic finite element material model for wood", *Composite Structures*, **50**, 143-149, (2000).
14. R.D. Cook, D.S. Malkus, and M.E. Plesha, "Concepts and applications of finite element analysis", New York: Wiley, 3rd edition, (1989).
15. M.G. Kollegal and S. Shridharan, "Compressive behavior of plain weave lamina", *Journal of Composite Materials*, **32**, 15, 1334-1355, (1998).
16. C. Chapman and J. Whitcomb, "Effect of assumed tow architecture on predicted moduli and stresses in plain weave composites", *Journal of Composite Materials*, **29**, 16, 2134-2159, (1995).
17. M. Karayaka and P. Kurath, "Deformation and failure behavior of woven composite laminates", *Journal of Engineering Materials and Technology*, **116**, 222-232, (April 1994).

Table 1. Failure criteria and degradation scheme for yarn material.

Failure mode	Failure condition	Discount coefficients				
		d_2	d_3	d_{f4}	d_{f5}	d_{f6}
Longitudinal tension	$c_t \sigma_1^y > X_t$	fiber breakage - ultimate failure				
Longitudinal compression	$-c_c \sigma_1^y > X_c$	fiber breakage - ultimate failure				
Transverse tension, 2-direction	$\sigma_2^y > Y_t$	0.01	1.00	0.20	1.00	0.20
Transverse compression, 2-direction	$-\sigma_2^y > Y_c$	0.01	1.00	0.20	1.00	0.20
Transverse tension, 3-direction	$\sigma_3^y > Y_t$	1.00	0.01	0.20	1.00	0.20
Transverse compression, 3-direction	$-\sigma_3^y > Y_c$	1.00	0.01	0.20	1.00	0.20
Longitudinal shear, 12-plane	$ \sigma_4^y > S_l$	0.01	1.00	0.01	1.00	1.00
Transverse shear, 23-plane	$ \sigma_5^y > S_t$	0.01	0.01	0.01	0.01	0.01
Longitudinal shear, 31-plane	$ \sigma_6^y > S_l$	1.00	0.01	1.00	1.00	0.01

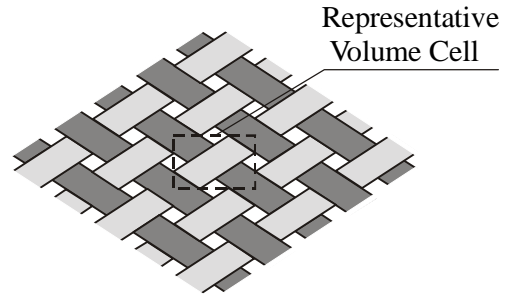


Fig. 1. Woven composite interlacing pattern.

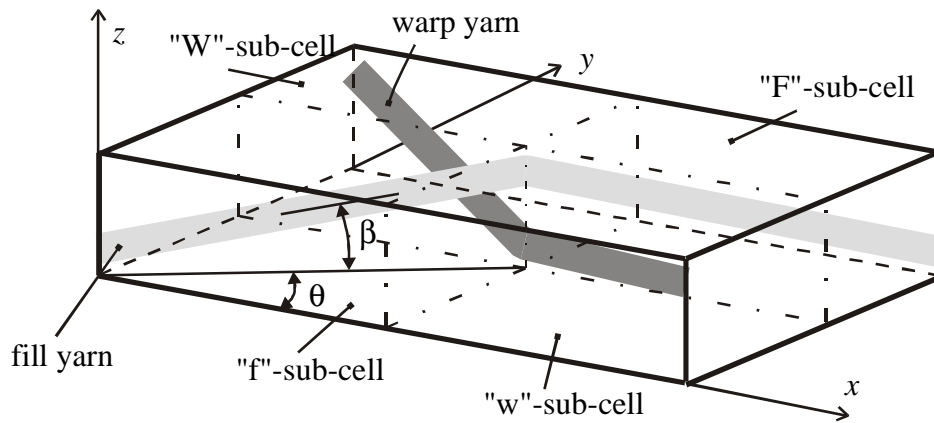


Fig. 2. Micro-mechanical model.

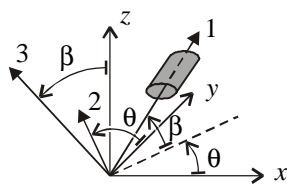


Fig. 3. Yarn orientation.

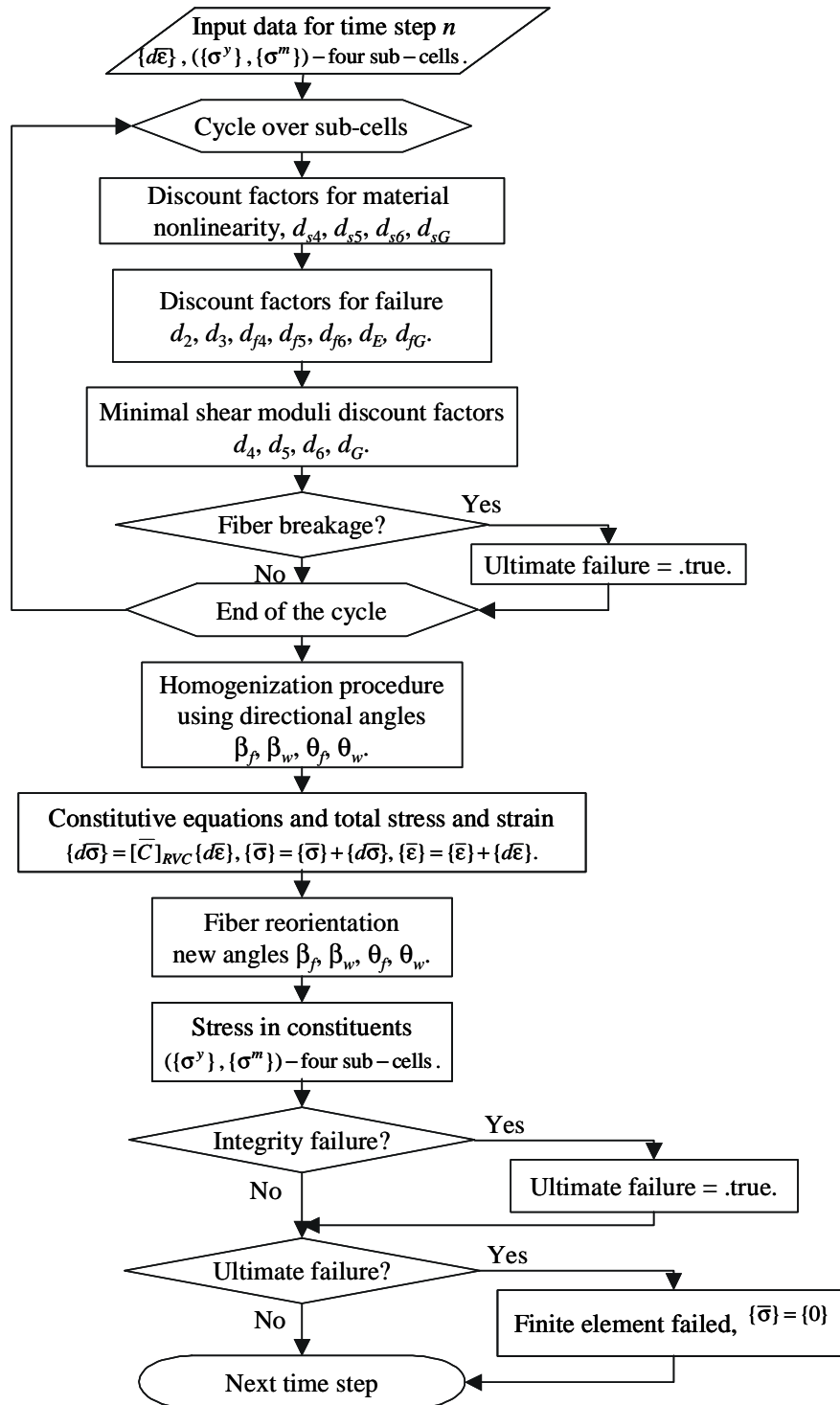


Fig. 4. Material model flowchart.

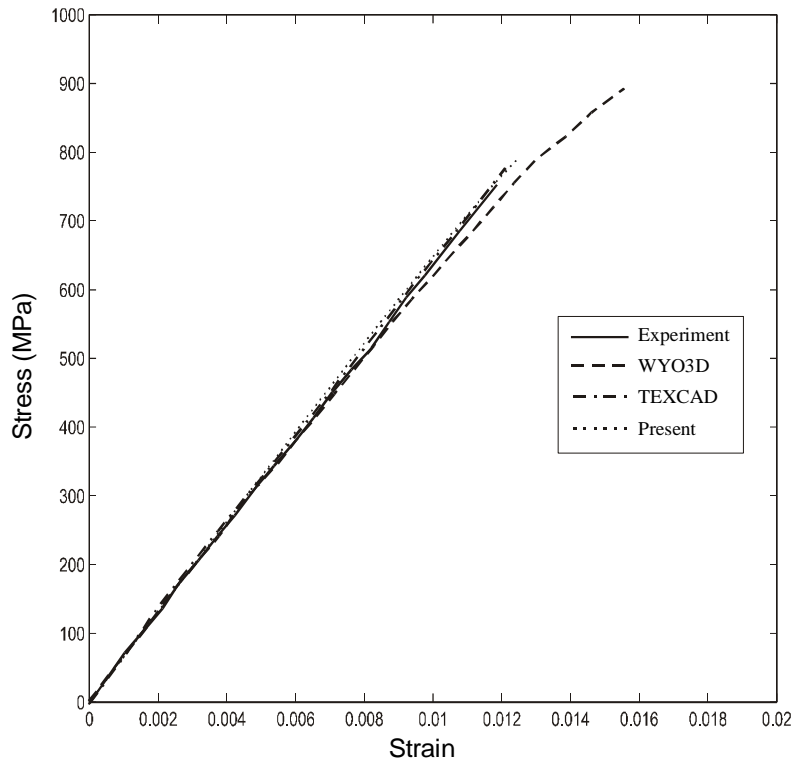


Fig. 5. Stress-strain response of the model in 0°/90° tension.

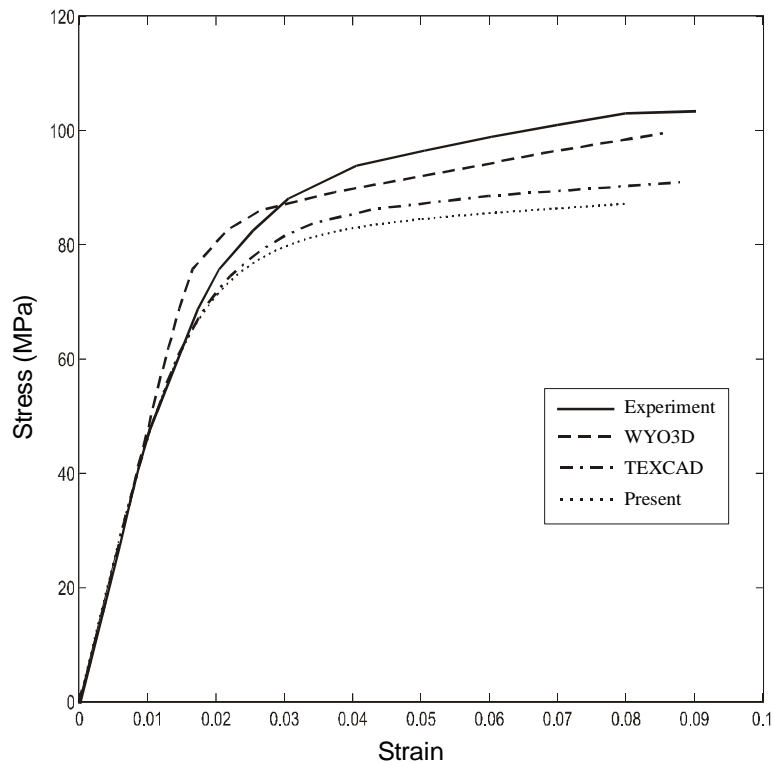


Fig. 6. Shear stress-strain response of the model in 0°/90° pure shear.

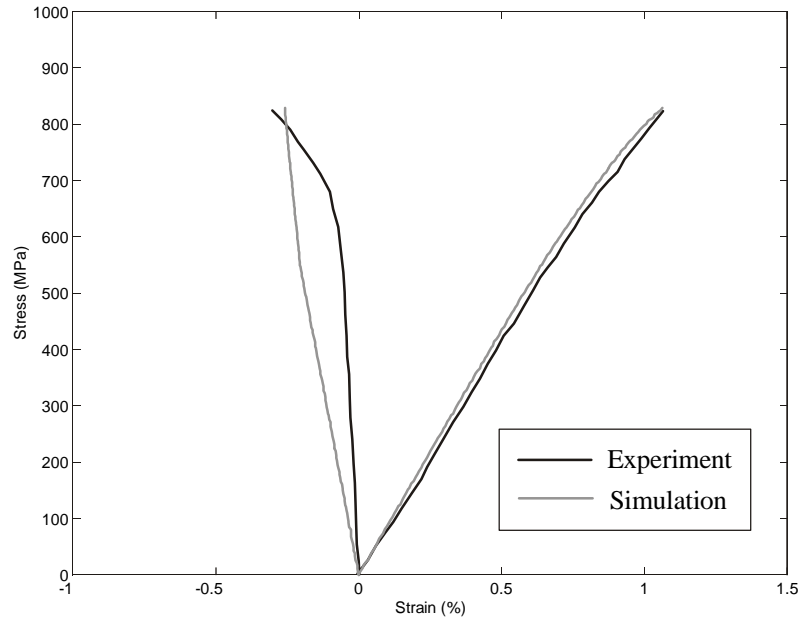


Fig. 7. Longitudinal stress vs. transverse and longitudinal strain in 0°/90° tension.

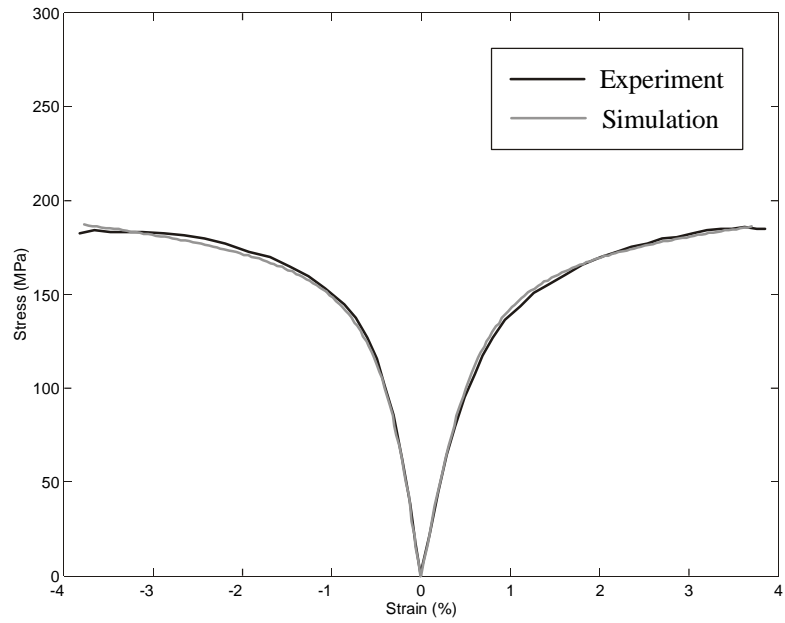


Fig. 8. Longitudinal stress vs. transverse and longitudinal strain in $\pm 45^\circ$ tension.

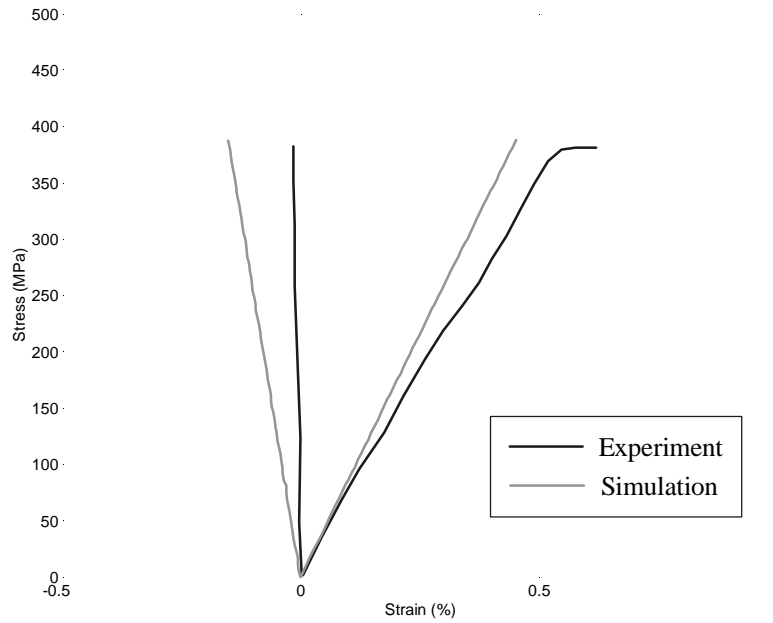


Fig. 9. Longitudinal stress vs. transverse and longitudinal strain in 0°/90° compression.

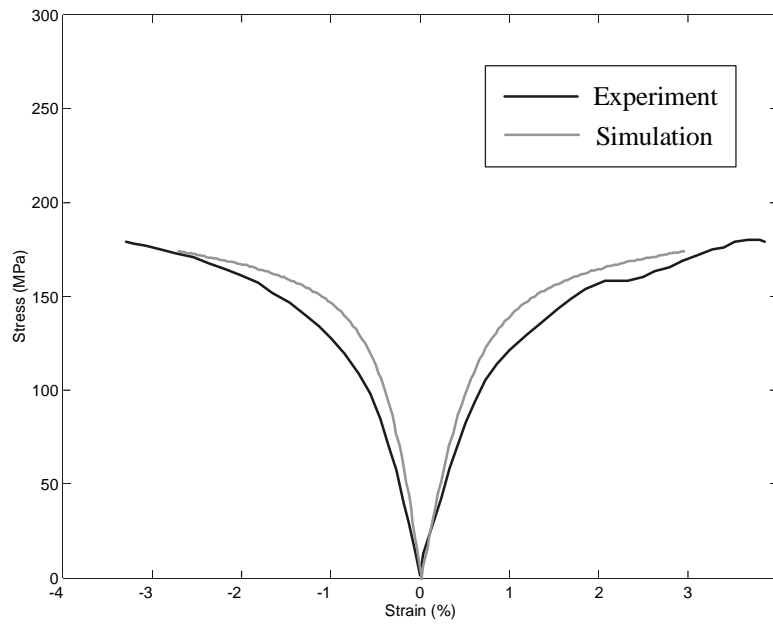


Fig. 10. Longitudinal stress vs. transverse and longitudinal strain in ±45° compression.

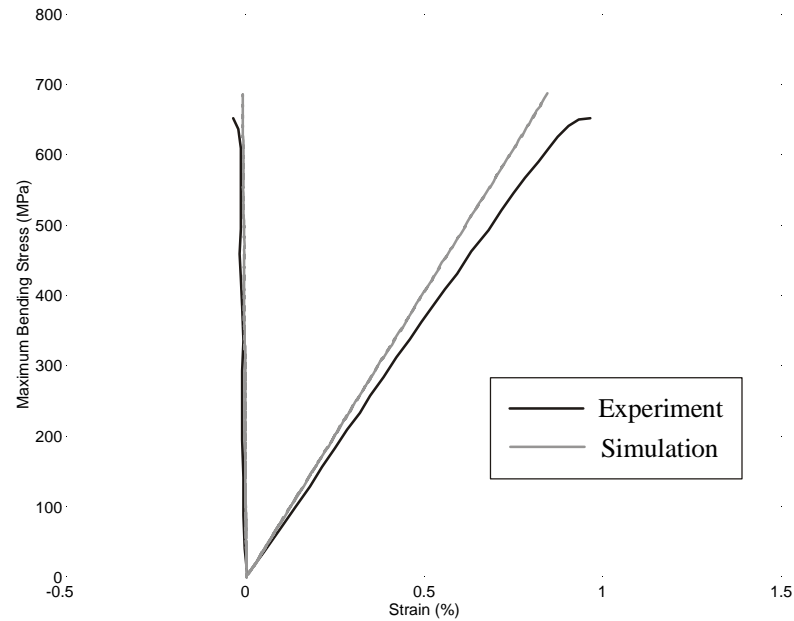


Fig. 11. Longitudinal stress vs. transverse and longitudinal strain in 0°/90° bending.

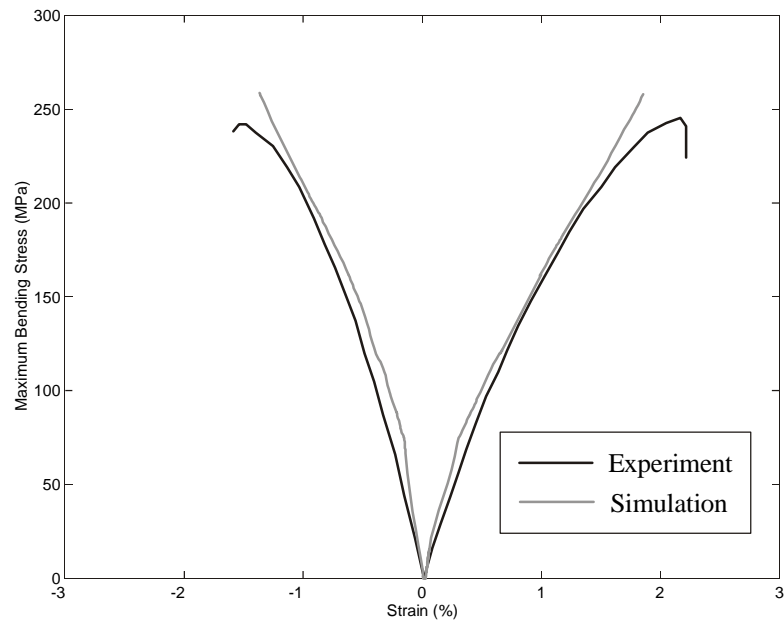


Fig. 12. Longitudinal stress vs. transverse and longitudinal strain in ±45° bending.

